

## Investigation of turbulence with wavelet bicoherence

**B.Ph. van Milligen**, E. Sánchez, T. Estrada, C. Hidalgo, B. Carreras<sup>1</sup>, L. García<sup>2</sup>

*Asociación EURATOM-CIEMAT, Madrid, Spain*

<sup>1</sup>*Oak Ridge National Laboratory, Oak Ridge, Tennessee, U.S.A.*

<sup>2</sup>*Universidad Carlos III, Madrid, Spain*

### Abstract

The analysis of nonlinear behaviour in turbulence requires special analysis tools since the usual linear analysis methods (e.g. spectral analysis) do not reveal all information. Here we investigate a recently introduced nonlinear tool for the analysis of turbulence: wavelet bicoherence [1,2]. It detects phase coupling (nonlinear interactions of the lowest -quadratic-order) with time resolution. In a model of drift wave turbulence, it detected a highly localized coherent structure associated with (but *not* located at) a rational surface, where the nonlinear coupling was reduced, perhaps due to a shear flow. Analyzing reflectometry measurements, it detected a strong increase in nonlinear phase coupling coinciding with the L/H transition.

### 1 Introduction: wavelet bicoherence

In turbulence studies, wavelet analysis is a valuable tool. It provides time-resolved information on the various scales (inverse frequencies) composing a signal. It removes a fundamental objection against Fourier analysis: the decomposition of a signal in 'harmonics' when the nonlinear equations describing turbulent phenomena do not possess harmonic eigenmodes.

The bicoherence, or the normalized bispectrum, is a measure of the amount of phase coupling that occurs in a signal or between signals [3,4]. Phase coupling occurs when two frequencies are simultaneously present in the signal(s) along with their sum frequencies, and the sum of the phases  $\phi$  of these frequency components remains constant. When the analyzed signal exhibits *structure* of any kind whatever, it might be expected that some phase coupling occurs. The generalization of the bispectrum to wavelet analysis may be expected to be able to detect temporal variations in phase coupling (intermittent behaviour) or short-lived structures.

### 2 Analysis of simulated data: A plasma drift wave turbulence model

The numerical results analyzed in this section correspond to a simple model of long-wavelength drift wave turbulence in sheared-slab geometry that was presented in [5]. The equilibrium quantities vary along the  $x$ -axis (radial direction) but are independent of the other two coordinates,  $y$  (poloidal), and  $z$  (toroidal). The equilibrium magnetic field is

$$\vec{B} = B_0 \left( \hat{z} + \frac{x}{L_s} \hat{y} \right), \quad (1)$$

where  $L_s$  is the magnetic shear length and  $\hat{y}$  and  $\hat{z}$  are the unit vectors in the  $y$  and  $z$  directions, respectively. In addition to the magnetic field, the equilibrium is characterized by the electron density and temperature profiles with basic scale lengths  $L_n$  and  $L_T$ , respectively.

The simplified drift wave model, valid for long wavelengths, is

$$\frac{d\tilde{n}_i}{dt} + V_{*n} \frac{d\tilde{n}_i}{dy} - L_n D_0 \left[ \vec{\nabla}_\perp \left( \frac{\partial \tilde{n}_i}{\partial y} \right) \times \hat{z} \right] \cdot \vec{\nabla}_\perp \tilde{n}_i + D_0 \frac{\partial^2 \tilde{n}_i}{\partial y^2} - \rho_s^2 \frac{d\nabla_\perp^2 \tilde{n}_i}{dt} - \frac{c_s^2}{v_i} \nabla_\parallel^2 \tilde{n}_i = 0. \quad (2)$$

The ion density is separated into averaged and fluctuating components. the fluctuating part of the density is indicated by a tilde and is written as a Fourier expansion:

$$\tilde{n}_i(x, \theta, \zeta) = \sum_{\substack{m,n \\ n>0}} \left[ \tilde{n}_{m,n}(x) \cos(m\theta + n\zeta) + \tilde{n}_{-m,n}(x) \sin(m\theta + n\zeta) \right] \quad (3)$$

here  $\theta$  and  $\zeta$  are the poloidal and toroidal angles, respectively, and are related to the  $y$  and  $z$  coordinates by  $y = x_0\theta$  and  $z = R_0\zeta$ . The poloidal and toroidal mode numbers are  $m = x_0k_y$  and  $n = R_0k_z$ , respectively. At the centre of the computational box of width  $a$ ,  $x = x_0$ . The boundary condition is that the density is zero at the conducting wall,  $x = x_0 - a/2$  and  $x = x_0 + a/2$ . We use finite differences in the radial coordinate  $x$ .

The equilibrium parameters for the nonlinear calculations are  $L_s/L_n = 20$ ,  $\rho_s/L_n = 3.6 \times 10^{-3}$ ,  $L_T/L_n = 1$ ,  $x_0 = 277\rho_s$ ,  $D_0 = 0.025\rho_s c_s$ , and  $D_\parallel = 2.4 \times 10^5 \rho_s c_s$ . The value of  $D_\parallel$  has been chosen to provide a range of unstable modes with  $6 \leq m \leq 76$ . The safety factor  $q$  is  $\frac{3}{2}$  at  $x = x_0$ . The standard box size is  $60\rho_s$ , and the number of unstable modes with resonant surfaces inside the computational box is about 250. In the calculation, we have included 439 Fourier components. The averaged density gradient is fixed, so saturation is caused by turbulence effects. The numerical data are for the saturated state.

Fig. 1 shows the RMS fluctuation level for this simulation, averaged over the time interval  $30.2 \times 10^4 < \Omega_i t < 40.4 \times 10^4$  (the time step, in these units, is 100), versus radius (given in units of  $\rho_s$ ). The RMS level peaks at the position of the  $q = \frac{3}{2}$  rational surface, associated with a resonant mode.

Fig. 2 shows the total bicoherence vs. radial position for this simulation. Note that (1) The bicoherence drops sharply at the position of the  $q = \frac{3}{2}$  rational surface, located at  $30 \rho_s$  (the RMS value nor the spectrum exhibit such a local drop). (2) The maximum of the bicoherence is at  $31 \rho_s$ . (3) Secondary maxima occur at positions that coincide roughly (but *not* exactly) with maxima in the RMS value (see Fig. 1). The major peak in bicoherence, though associated with the mode at  $q = \frac{3}{2}$ , is slightly shifted with respect to the rational surface. We conclude that the bicoherence provides information that pertains to an aspect of the turbulence (non-linear, or rather quadratic behaviour) that is not captured by either the RMS or the spectral analysis.

Fig. 3 shows the cross correlation, the weighted average cross coherence and the weighted average cross phase between one radial position and the next; the weighting being done by the spectral power. The cross correlation and cross coherence between adjacent radial

positions are generally high, but drop around  $30 \rho_s$ , and the cross phase peaks around  $30.5 \rho_s$ , possibly indicating shear flow. The numerical results also show the existence of a shear flow layer in this location. This seems to suggest an explanation of the drop in bicoherence at  $30 \rho_s$  in terms of a decorrelation of the turbulence, possibly linked to a shear flow.

The maximum in the bicoherence at  $31 \rho_s$  is related to the presence of a long-living structure that is highly localized poloidally and radially. It has the (3,2) periodicity and lies close to the  $q = \frac{3}{2}$  surface; and is indeed visible in a two-dimensional plot of the ion density.

### 3 Observation of L/H transition on Wendelstein VII-AS

We have analyzed data taken with a broadband X-mode heterodyne reflectometer [6] in the edge of the Wendelstein VII-AS modular, low-shear stellarator with major radius  $R_0 = 2$  m and minor radius  $a \approx 0.18$  m [7]. The toroidal magnetic field is  $B = 2.5$  T. The plasma was heated with  $P_{ECH} = 400$  kW of ECRH power at 140 GHz. The central electron density and temperature were  $n_e = 8 \times 10^{19} \text{ m}^{-3}$  and  $T_e = 0.8$  keV. The edge rotational transform was  $\iota = 0.53$ . We studied the L/H transition, common in this kind of discharges [8], and always accompanied by a sudden reduction in the measured fluctuation levels of e.g. the electron density.

Data are taken at a radial position of about 15.5 cm, which is where the strongest reduction in the fluctuation level is observed during the L/H transition. This position is about 1 cm inside the separatrix. Fig. 4 shows the time development of the total bicoherence and of the RMS level of the reflectometry data, as well as the signal from the  $H_\alpha$ -light emission detector. A sharp drop in the signal from the  $H_\alpha$  detector is generally considered to be indicative of an L/H transition. The transition is seen to occur at 757.5 ms. Observe that the L/H transition is clearly seen both on the total bicoherence and RMS signals. Before the transition, the RMS value is high and the bicoherence is at noise level (dashed line). In the H-phase the bicoherence is clearly augmented (by a factor 2-3), whereas the RMS level has dropped by a similar factor.

### Acknowledgements

This work was made possible by Commission of the European Communities Bursary ERB4001GT921485. The authors thank their colleagues at Wendelstein for sharing their data with us and their colleagues at the Asociación EURATOM-CIEMAT for a pleasant cooperation.

### References

- [1] B. Ph. van Milligen, C. Hidalgo and E. Sánchez, Phys. Rev. Lett. **74**, 3 395 (1995)
- [2] B.Ph. van Milligen, E. Sánchez, T. Estrada, C. Hidalgo, B. Brañas, B. Carreras, L. García, Accepted for publication in Plasma Physics (1995)
- [3] Y.C. Kim, J.M. Beall and E.J. Powers, Phys. Fluids **23** (2) 258 (1980)
- [4] Ch. P. Ritz, E.J. Powers and R.D. Bengtson, Phys. Fluids **B 1** (1) 153 (1989)

- [5] B.A. Carreras, K. Sidikman, P.H. Diamond, P.W. Terry and L. Garcia, Phys. Fluids B **4** (10) 3115 (1992)
- [6] H.J. Hartfuß, T. Estrada, M. Hirsch, *et al.*, Rev. Sci. Instrum. **65** (7) 2284 (1994)
- [7] H. Renner, *et al.*, Plasma Phys. Controlled Fusion **31** 1579 (1989)
- [8] V. Erckmann, F. Wagner, J. Baldzuhn, *et al.*, Phys. Rev. Lett. **70** 2086 (1993)

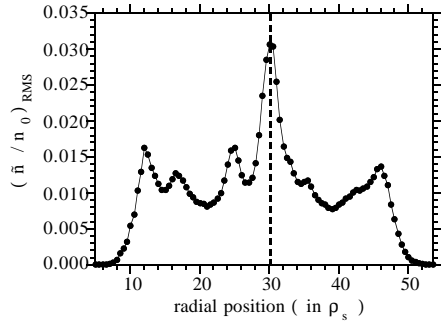


Fig. 1 - RMS fluctuation level vs. radius of the ion density in the sheared slab drift wave model discussed in the text.

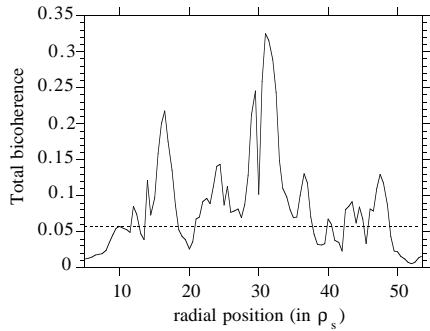


Fig. 2 - Total wavelet bicoherence vs. radial position for the same data as in Fig. 1.

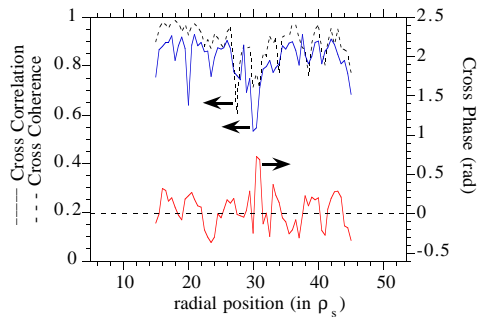


Fig. 3 - Cross correlation, cross coherence, and cross phase between adjacent channels. Results are shown at position  $x \rho_s$  for the cross analysis between  $x \rho_s$  and  $(x+0.5) \rho_s$ . The cross coherence and -phase are computed from FFT (cross) spectra and averaged over all frequencies by weighing with the spectral power.

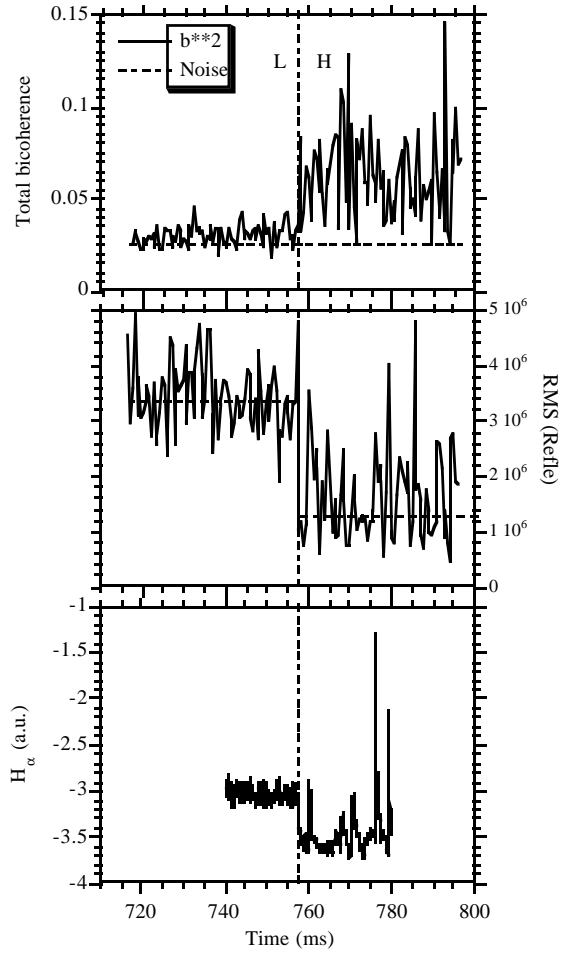


Fig. 4 - Plots of the total bicoherence and RMS of the reflectometry signal taken at Wendelstein VII-AS, and the fast  $H\alpha$  signal. The L/H transition is marked by a vertical dashed line and shows up clearly in all graphs.